THE BELL SYSTEM TECHNICAL JOURNAL
Vol. 57, No. 6, July–August 1978
Printed in U.S.A.

Atlanta Fiber System Experiment:

Optical Detector Package

By R. G. SMITH, C. A. BRACKETT, and H. W. REINBOLD

(Manuscript received February 10, 1978)

The optical detector package used in the Atlanta Fiber System Experiment is described. The detector subsystem consists of an avalanche photodetector and a transimpedance amplifier packaged in a dual in-line configuration, with a connectorized optical-fiber pigtail for optical interfacing. We describe here the design, operation, and construction of the amplifier circuit, the gain and noise characteristics of the avalanche photodetector, and the experimental performance of 53 completed packages. The design is found to meet or exceed all system performance goals. The measured performance of the 53 subsystem packages gives an average optical sensitivity of −54.1 dBm (BER = 10^{-9}) with a standard deviation of 0.28 dB, a transimpedance of 13.7 kΩ, a dynamic range of 76 dB (38 dB of optical power), an effective quantum efficiency of 69 percent, and a frequency response corresponding to complex poles located at −70 ± j56 MHz. The optical sensitivity was found to be unchanged within experimental error when measured at 50°C. Preliminary life testing of 32 units, 10 of which are operating at 60°C, has produced no failures in over 7×10^5 equivalent device hours. These are very encouraging results and imply a device reliability approaching that required for system applications.

I. INTRODUCTION

This paper describes the design, packaging, and performance characteristics of the optical detector packages used in the receiver portion of the regenerator employed in the Atlanta Fiber System Experiment recently completed in Atlanta, Georgia.

The goal of this development effort was to design a self-contained optical detector package containing the photodetector along with the associated preamplifier which would operate at the DS3 transmission

rate (44.7 Mb/s), achieve good sensitivity, possess a wide dynamic range, and be easily interfaced both optically and electrically to the printed circuit board and backplane. The design was also to produce a level of performance representative of a manufacturable unit. This latter constraint affected several of the engineering choices made during this development.

The optical detector package, to be described in detail below, employs an avalanche photodiode as the optical detector and a transimpedance amplifier as the interface between the detector and the remainder of the linear channel. The combination is enclosed in an EMI shield and potted in plastic to provide mechanical rigidity. Optical interfacing is accomplished by use of a short piece of optical fiber connected on one end to the APD and on the other end to an optical connector. Electrical interfacing is achieved via pins designed to fit either into a socket or on to a printed circuit board.

The performance of 53 detector packages fabricated and evaluated for this project includes a measured optical sensitivity of −54.1 dBm with a standard deviation of 0.3 dB for a bit error rate of 10^{-9} and a dynamic range of 38 dB of optical power compared to design goals of −53 dBm and 30 dB, respectively. Measured performance at 50°C showed no degradation from room temperature results.

II. CIRCUIT DESCRIPTION

The front end of an optical receiver consists of a photodetector, generally a PIN or avalanche photodiode, along with some form of amplifying stage or stages. The overall combination of the detector, amplifier, and subsequent filtering is designed to respond to the input light signal in such a way as to provide an output pulse shape—usually with a raised cosine spectrum—appropriate for presentation to the digital decision circuit. The combination, referred to as the linear channel, must therefore have sufficient bandwidth to respond properly to the input pulse. It should also contribute as little noise as possible in order to give a good optical sensitivity.

A number of approaches to the design of the input amplifier or front end have been investigated. The most straightforward method is to terminate the detector in a load resistor, R, chosen such that in combination with the input capacitance of the amplifier, C, the RC time constant is sufficiently small to reproduce the input pulse shape. This approach, though straightforward, has been shown to be excessively noisy.[1-3]

An alternative to this approach, usually referred to as the high impedance or integrating front end, used extensively in nuclear engineering, has been analyzed in detail by Personick.[1] He shows that it has less noise and results in considerable improvement in optical sensitivity compared

to the technique discussed above. Receivers have been designed and built using integrating front ends, verifying the predicted noise reduction and sensitivity improvement.[2,3]

The essential feature of the design of a low-noise front end is minimizing the contributions of the various sources of noise, including those resulting from leakage currents in the photodiode, thermal noise associated with biasing resistors, and noise associated with the amplifying transistors. If the input signal source is a photodiode, which looks like a current source shunted by a capacitor,[4] minimizing the noise is accomplished by increasing the values of biasing resistors, reducing all associated capacitances, and minimizing leakage currents.[1] For a bipolar transistor, choice of an optimum collector current is also required.[5] Such an optimization results in an amplifier which has a bandwidth considerably smaller than that required to reproduce the desired pulse shape. This situation is remedied by subsequent equalization which can be performed with little or no noise penalty.

Although this approach has been shown to give optimum performance, there are several drawbacks. First of all, the degree of equalization will depend upon the parasitics of the circuit. This introduces the possibility that circuits would require equalization on an individual basis—an undesirable step from a manufacturing point of view. The most serious drawback, however, is the loss of dynamic range resulting from the equalization.[6]

A third approach, and the one employed here, is to use a shunt feedback amplifier, commonly referred to as a transimpedance amplifier, which is essentially a current-to-voltage converter. A simplified diagram of the transimpedance amplifier is shown in Fig. 1. In the limit of large gain, the output voltage, V_o, is related to the input current, i, by the relation

$$V_o = -Z_F i, \tag{1}$$

where Z_F is the feedback impedance.

The feature of the transimpedance amplifier that makes it desirable for the present use is that, compared to an unequalized amplifier that does not employ feedback, it is less noisy for a given bandwidth or alternatively has more bandwidth for a given noise level. Compared to an

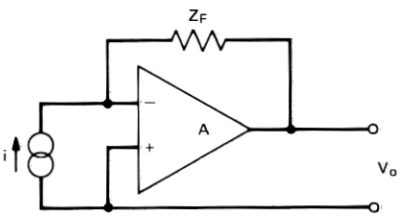

Fig. 1—Schematic representation of the transimpedance amplifier.

optimized, equalized amplifier of the high impedance design, a receiver employing the transimpedance amplifier along with an avalanche photodetector requires approximately 1 dB more optical power to achieve a given error rate. Circuit simplicity, eliminating the need to employ equalization, and obtaining increased dynamic range were judged worth the 1-dB loss in sensitivity.

A schematic diagram of the transimpedance amplifier used here is shown in Fig. 2. The first two transistors comprise the feedback pair or transimpedance portion of the circuit; the third stage provides additional gain and isolation. Q_1 was chosen to have as small an input capacitance as possible and was selected to have a high β. Q_2 and Q_3 were unselected devices of the same type, chosen for commonality in bonding technique. A tendency of early circuits to oscillate was eliminated by using a resistance in the base of Q_2. Other components shown in Fig. 2 are used for filtering and bypassing.

The basic transimpedance of the feedback pair is approximately given by the feedback resistor, in this case, 4 kΩ. To increase the output signal level to 4 mV peak to peak at the minimum optical signal level, the gain of the third stage was chosen to be 3.7, giving an effective transimpedance of 14.8 kΩ.

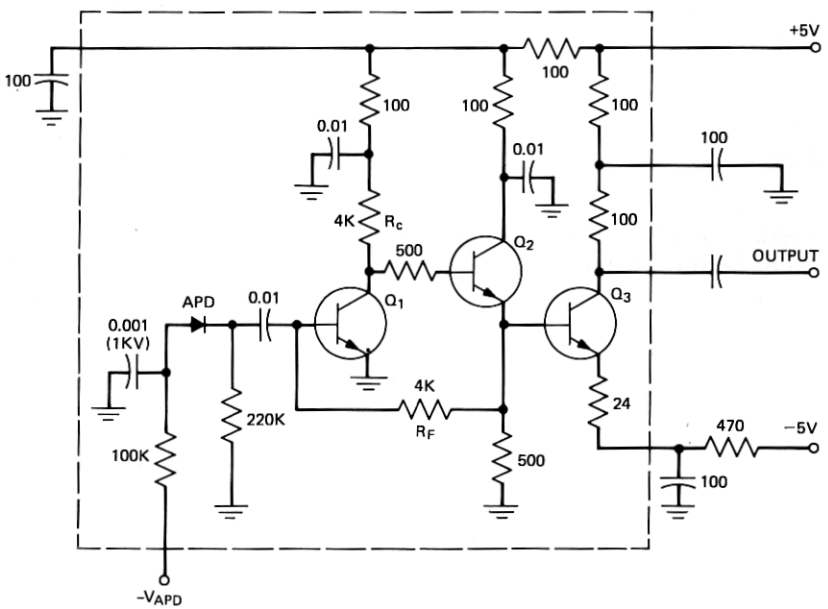

Fig. 2—Circuit diagram of the amplifier used. Components shown within the dotted line are included within the package.

III. AVALANCHE PHOTODIODE

The photodetector used in the optical detector package is an avalanche photodiode (APD). This detector, designed and developed for this application, is described in a companion paper.[7] The essential feature of the avalanche photodiode is that it provides internal multiplication of the photo-generated current that improves the sensitivity of the receiver.

A typical gain-versus-voltage curve for the avalanche photodetectors used is shown in Fig. 3. The important features of this curve are the rapid increase in the gain with voltage near 50 V reverse bias and again near 400 V. The first region is associated with the depletion of the device, the second with approach to self-sustained avalanche breakdown. The device must be operated at a voltage in excess of that required to deplete the π region in order to obtain adequate speed of response and below self-sustained breakdown where the device is excessively noisy. More specifically, the devices used here could operate with a minimum gain of approximately 6, at which point they were sufficiently fast, and were capable of producing gains in excess of 100. (As discussed later, the optimum gain was found to be 80.)

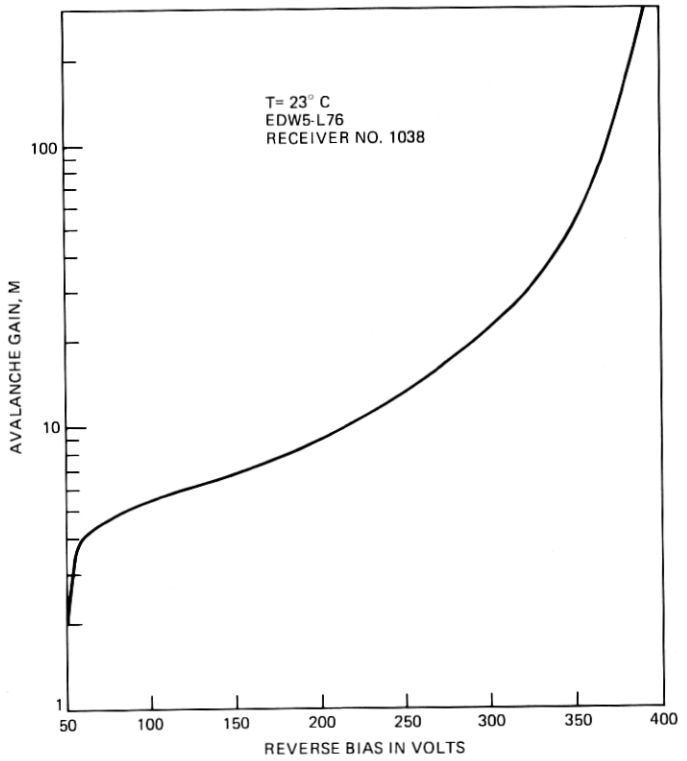

Fig. 3—Room temperature gain curve of an avalanche photodiode typical of those used in the detector packages.

The gain of the avalanche photodiode is temperature-dependent, requiring approximately 1.5 V per °C increase in bias voltage to achieve constant gain. To compensate for temperature variations and for varying input light levels, the bias to the diode, which is generated by an up-converting power supply located on the main board, is controlled by a feedback loop which maintains the signal level at the output of the linear channel at a constant value.[8] The range over which the APD gain is varied extends from a minimum value of approximately 6 (at high light levels) to 80 (corresponding to an error rate of 10^{-9} at the minimum detectable optical power level). Further discussion of the operation of the gain control of the linear channel may be found in Ref. 8.

IV. PACKAGE DESIGN

The physical design of the optical detector package was approached with the goal of designing a unit that would be physically sturdy and that could be easily interfaced with the circuit board and backplane both electrically and optically. Electrical interfacing was achieved using a standard electrical pin configuration to permit the package to be plugged into a socket on the printed circuit board. Optical interfacing was achieved through the use of an optical pigtail—a short piece of optical fiber protected by a plastic sheath—placed in proximity to the APD on one end with a molded optical connector on the other end. Fig. 4 is a photograph of the completed package.

In this design, the APD and the optical pigtail were packaged as a subassembly, and this subassembly was later attached to the ceramic circuit board. This approach was taken to simplify the package development and to permit separate testing of the APD and circuit. More recent packaging approaches coupled with improved circuit design have resulted in a detector package with the APD chip mounted directly to the circuit board, yielding a more compact package with improved performance.

The amplifier circuit was fabricated using thick-film technology. The transistors used were beam-lead, sealed-junction devices that were thermocompression-bonded to the thick-film circuit. The ceramic circuit board with the APD subassembly attached was placed within an EMI shield, and the entire assembly was potted in plastic to provide mechanical rigidity to the electrical pins and the optical pigtail.

V. PERFORMANCE CHARACTERISTICS

During the course of this development, approximately 100 detector packages were fabricated; of these, 53 were characterized in detail. The results and comparison with theory, where appropriate, are summarized below.

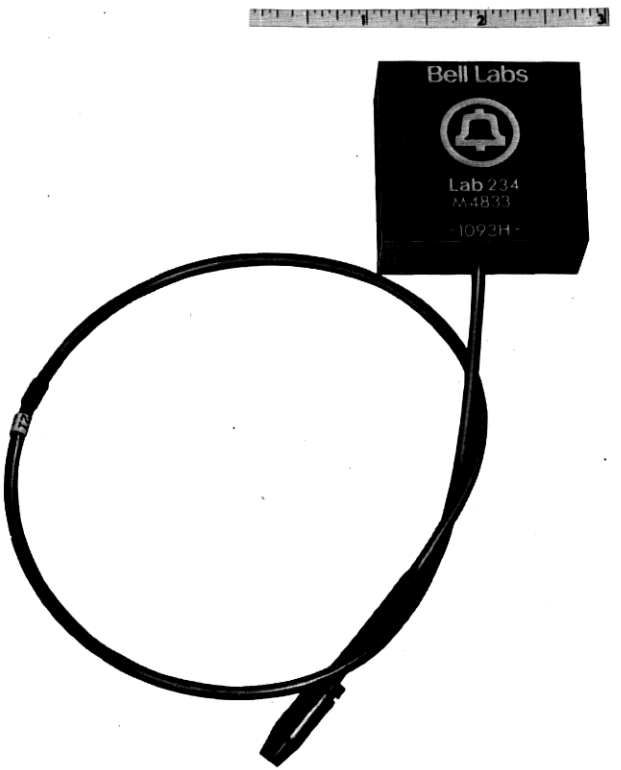

Fig. 4—Finished optical detector package.

5.1 Equivalent input noise current density

The optical sensitivity of an optical receiver is determined primarily by the equivalent input noise current density of the detector-amplifier combination and the avalanche characteristics of the APD. For a transimpedance amplifier of the type used here, there are several principal sources of noise including: (*i*) thermal noise of the feedback resistor, R_F, (*ii*) shot noise of the base current of Q_1, (*iii*) shot noise associated with the collector current of Q_1, and (*iv*) leakage currents in the photodetector. The APD used here was designed to minimize leakage currents and in all cases, even at elevated temperatures, noise associated with surface leakage and bulk dark currents was completely negligible. Further, for the collector current used in Q_1, the contribution from (*iii*) is expected to be small. The dominant noise sources for the present circuit

are thus the feedback resistor and the base current of Q_1. For these noise sources, the spectral density of the equivalent input noise current will be flat and is given by

$$\frac{d}{df}\langle i^2\rangle = \frac{4kT}{R_F} + 2qI_B, \tag{2}$$

where

k = Boltzmann's constant
T = absolute temperature
q = electronic charge
I_B = base current of Q_1
R_F = feedback resistor.

Using $R_F = R_C = 4$ kΩ and $V_{cc} = 5$ V, eq. (2) reduces to

$$\frac{d}{df}\langle i^2\rangle = 4.14 \times 10^{-24}\left(1 + \frac{70}{\beta}\right), \tag{3}$$

where $\beta = I_C/I_B$ and T is taken to be 300 K. Taking $\beta = 150$, a typical value for the transistors used, eq. (3) has a value of 6.07×10^{-24} A^2/Hz.

The above noise current density is, by assumption, independent of frequency. The actual frequency dependence was determined by measuring the output noise spectral density with a spectrum analyzer, referring this to the input using the measured frequency response of the amplifier. The results are shown in Fig. 5, where the noise is found to be flat out to approximately 20 MHz with a 3-dB corner frequency of 87.5 MHz. When the frequency response of the filter used to limit the noise and shape the pulse is taken into account (the system response is down 10 dB at 40 MHz and 20 dB at 54 MHz), the contribution to the total output noise from the frequency dependent portion is found to be negligible. Thus, assuming a flat equivalent noise spectral density at the input introduces little error in receiver sensitivity calculations.

The absolute magnitude of the input noise spectral density was determined by measuring the total output noise power (after the filter, using a true rms power meter) and referring this to the input using known amplifier gains, the measured transimpedance, and the measured characteristics of the filter. The resultant mean input noise current density was found to be 6.92×10^{-24} A^2/Hz. The difference of 0.6 dB between the measured and calculated values may be due in part to noise sources that have been neglected, but a significant contribution is believed due to uncertainties in the determination of the transimpedance.

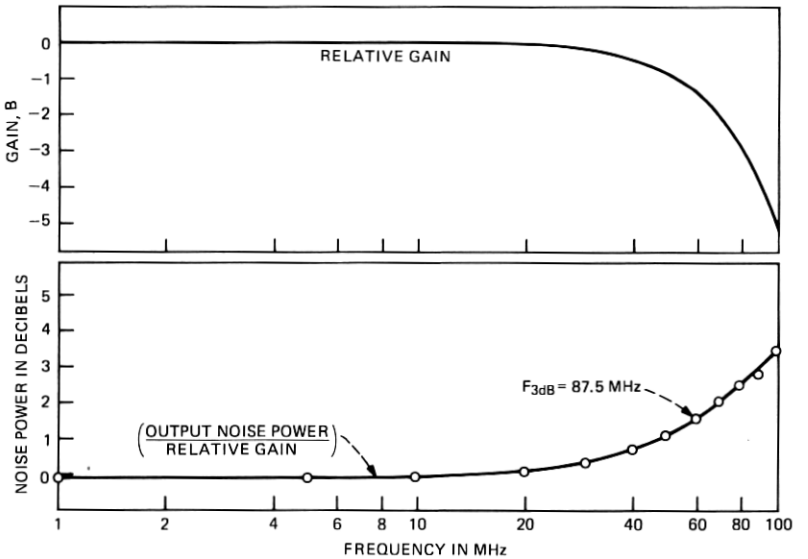

Fig. 5—Plots of relative gain and effective input noise current density as functions of frequency.

5.2 Receiver sensitivity

The sensitivity of an optical receiver is given by[2]

$$\eta\overline{p} = h\nu \frac{Q}{2}\left[\frac{Q\langle M^2\rangle B}{M^2} + \frac{2}{qM}(\langle i^2\rangle)^{1/2}\right], \tag{4}$$

where

η = the overall quantum efficiency of the diode and coupling structure

$\overline{p}$ = the average optical power required to achieve a given bit error rate (BER), assuming an equal population of ones and zeros

Q = a function of the bit error rate; $Q \cong 6$ for BER $= 10^{-9}$

$h\nu$ = energy of a photon $\approx 2.4 \times 10^{-19}$ J

q = electronic charge $= 1.6 \times 10^{-19}$ coulomb

B = bit rate (assuming the two-level coding)

$(\langle i^2\rangle)^{1/2}$ = root-mean-square noise current of the amplifier referred to the input

$M = \langle M\rangle$ = average avalanche gain

$\langle M^2\rangle = \langle M\rangle^2 F(M)$ = mean square avalanche gain

$F(M)$ = excess noise factor associated with the avalanche process.

Equation (4) has been derived assuming that the noise in the zero state

is independent of the signal level and that the noise has a Gaussian amplitude distribution.

For a given bit rate, B, and error rate determined by Q, the average optical power required to achieve the error rate is a function of the average avalanche gain, $\langle M \rangle$, and the excess noise factor, $F(M)$. The excess noise factor, $F(M)$, is given by[9]

$$F(M) = M\left[1 - (1-k)\left(\frac{M-1}{M}\right)^2\right], \tag{5}$$

where k is an effective ratio of the ionization coefficients of holes and electrons in the avalanche region. For the devices used here, $k \approx 0.035$ for a front-illuminated diode and a wavelength of 825 nm.[10] The value of $\eta\bar{p}$ required to achieve an error rate of 10^{-9} ($Q = 6$) as determined from eqs. (4) and (5) is plotted in Fig. 6 as a function of M, using the average measured input noise current, $(\langle i^2 \rangle)^{1/2} = 1.45 \times 10^{-8}$ A. The curve indicates that the sensitivity is maximum for an avalanche gain of approximately 140 with an optimum value $\eta\bar{p} = -56.6$ dBm. The sensitivity for $M = 1$, corresponding to a p-i-n diode is -38.9 dBm. Also shown by the cross in the figure is the average measured sensitivity of 53 devices taken at an avalanche gain of 80. This value of gain was found to yield the optimum sensitivity as constrasted to the predicted value of ≈ 140. The optimum value of threshold for the decision circuit was found to be approximately 45 percent of the peak eye height in contrast to a considerably smaller value predicted by the theory.

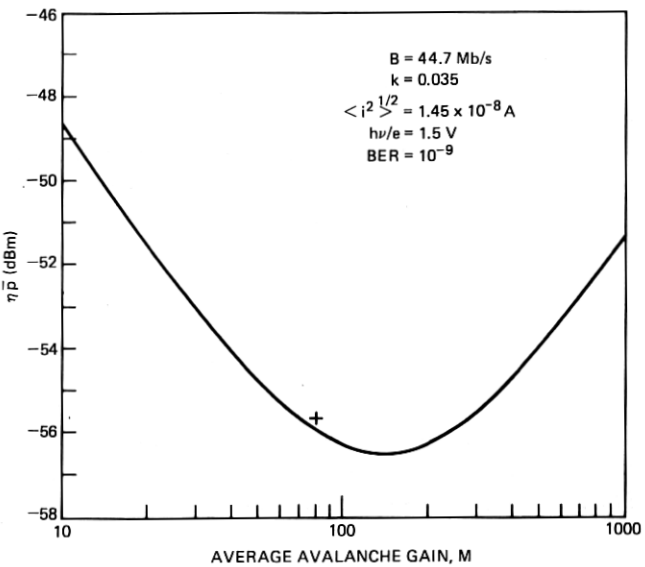

Fig. 6—Plot of the calculated optical sensitivity as a function of the average avalanche gain, M. The cross represents the average of the measured sensitivity of 53 receivers.

The primary reason for the above deviations is associated with the fact that the amplitude distribution of avalanche gain is not Gaussian, but is skewed toward higher gain values.[11–14] This has the effect of greatly enhancing the effective noise generated by current associated with the zero state of the incident light (determined by the extinction ratio of the source[15]). The rapid increase of this noise with avalanche gain effectively limits the extent to which the decision level can be lowered and hence reduces the optimum avalanche gain. Sensitivity calculations incorporating the non-Gaussian nature of the avalanche gain do, in fact, predict an optimum gain very close to the value of 80 determined here.[13] The measured sensitivity is seen to be in close agreement with that calculated from eq. (4) at a gain of 80.

A plot of the distribution of measured values of $\eta\bar{p}$ is shown in Fig. 7b. The mean value is −55.7 dBm with a standard deviation of 0.22 dBm.

5.3 Quantum efficiency

The sensitivity discussed above is expressed in terms of the product of the quantum efficiency, η, and the average optical power, $\bar{p}$. This is a convenient means of characterizing the sensitivity of receivers, as it requires only a measurement of the current drawn by the photodetector and a knowledge of the avalanche gain; it is not necessary to measure optical power, which can be difficult at such low power levels. By measuring the optical power, it is possible to determine $\bar{p}$ and thus to infer the quantum efficiency, η. A plot of the measured values of $\bar{p}$ is shown in Fig. 7a. The mean value is −54.1 dBm with a standard deviation of 0.28 dBm. Comparing the mean values for $\bar{p}$ and $\eta\bar{p}$, the mean quantum efficiency is calculated to be −1.6 dB, or 69 percent. Contributing to this value are coupling losses within the pigtail structure as well as the intrinsic quantum efficiency of the diode, which was typically 90 percent.

5.4 Temperature effects

The sensitivities of the optical detector packages were measured at

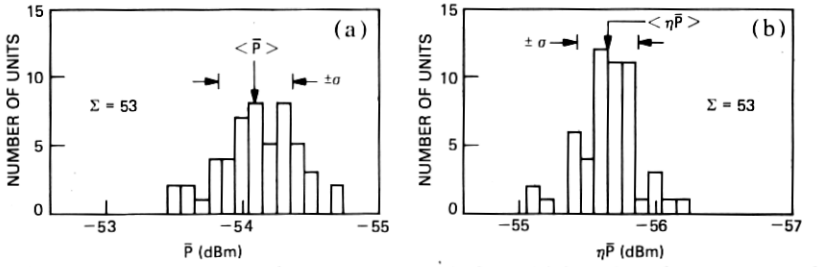

Fig. 7—Plots showing the distribution of optical sensitivities for a bit error rate of 10^{-9}.

50°C as well as at room temperature. Within ±0.1 dBm, and well within experimental error, the measured values were found to be the same at the two temperatures. There is thus no evidence of degradation in performance, at least to 50°C.

5.5 Pole locations

In the initial design of the amplifier, it was not known how accurately the pole locations could be controlled. It was thus decided to design the amplifier with sufficient bandwidth that any variations in its frequency response characteristics would not significantly affect the overall response of the linear channel including the final filter. The resulting amplifier design thus had a bandwidth in excess of that required for operation at 45 Mb/s, and its noise was correspondingly higher.

The frequency response of the detector package was measured by illuminating the APD with incoherent light and measuring the output noise spectrum with a spectrum analyzer. When the spectral density of the shot noise of the APD is much larger than that of the amplifier noise, the output noise is proportional to the amplifier response function. This response function was fitted, using a least-squares method, to a two-pole transfer function. The resulting pole locations were found to be complex with a mean value of $-70 \pm j56$ MHz. Although the poles are complex, they are sufficiently removed from the poles of the filter to have little effect on the overall system response. In amplifier designs performed subsequent to this development, careful attention to the reduction of parasitics has resulted in amplifiers with real poles and bandwidths in excess of those reported here.

5.6 Power supply requirements

The circuit was designed to operate from nominal +5 V, −5.2 V power supply voltages. No variation in performance of the detector package was observed for variations of ±1 V about these nominal values.

5.7 Dynamic range

One of the principal reasons for choosing the transimpedance design was to obtain a large dynamic range. The dynamic range of the amplifier is defined as the ratio of the maximum output voltage swing to the value when the receiver is operating at maximum sensitivity. For an error rate of 10^{-9}, $\eta\bar{p} = -55.7$ dBm and using $M = 80$, the peak input current to the amplifier is calculated to be 0.29 μA. With a measured transimpedance of 13.7 kΩ, the output voltage is 4 mV p-p. The maximum output voltage swing is found to be ±0.9 V, limited by the third-stage biasing and the use of ac coupling of the APD to the amplifier. The resultant dynamic range is then 53 dB electrical, or 26.5 dB of optical power.

The overall dynamic range of the optical detector package includes the range of available gain of the APD as well as the dynamic range of the amplifier. The ratio of the optimum gain ($M = 80$) to the minimum value where the device becomes slow ($M \cong 6$) gives an additional contribution to the dynamic range of 22.5-dB electrical or 11.3-dB optical. The overall dynamic range of the optical detector package is then approximately 76-dB electrical or 38-dB optical power, compared to a design goal of 30-dB optical power.

VI. SUMMARY

An optical detector package consisting of a silicon avalanche photodetector and a low-noise amplifier has been developed for experimental studies of a fiber-optic system operating at 45 Mb/s. The self-contained unit has been designed to plug into a printed wiring board and to interface optically via a connectorized optical pigtail.

The performance of the unit is characterized by an optical sensitivity of −54.1 dBm at a bit error rate of 10^{-9}, with a dynamic range in excess of 38 dB of optical power. Both values exceed the nominal specifications placed on the units. The range of measured sensitivities showed a rather tight standard deviation of 0.28 dBm, and performance was unchanged over the temperature range of 20°C to 50°C.

A number of units of this design have been successfully operated in the Atlanta Experiment and are currently being used in a field evaluation now under way in Chicago, Illinois.

VII. ACKNOWLEDGMENTS

The development of the detector package described here involved the contributions of many people within Bell Laboratories. In addition to those involved in the development of the avalanche photodiode, described in a companion paper, the authors wish to thank T. C. Rich for the package design; H. M. Cohen, W. B. Grupen, B. E. Nevis, E. L. Soronan, and A. E. Zinnes for supplying the thick-film circuits; M. M. Hower, F. M. Ogureck, and Tseng-Nan Tsai for providing transistors; A. W. Warner and W. W. Benson for supplying the fiber pigtails; M. F. Galvin, R. P. Morris, and J. R. Potopowicz for their excellent technical assistance; and D. P. Hansen and S. W. Kulba for fabricating the packages. The authors would like to express appreciation to G. L. Miller for many stimulating discussions and M. DiDomenico for his encouragement throughout the project.

REFERENCES

1. S. D. Personick, "Receiver Design for Digital Fiber Optic Communication Systems, Parts I and II," B.S.T.J., *52*, No. 6 (July–August 1973), pp. 843–886.
2. J. E. Goell, "An Optical Repeater With High-Impedance Input Amplifier," B.S.T.J., *53*, No. 4 (April 1974), pp. 629–643.

3. P. K. Runge, "An Experimental 50 Mb/s Fiber Optic PCM Repeater," IEEE Trans. Commun., *COM-24* (April 1976), pp. 413–418.
4. H. Melchior, *Laser Handbook*, Arecchi and Schulz-DuBois, eds., Amsterdam: North Holland, 1972, pp. 727–835.
5. J. E. Goell, "Input Amplifiers for Optical PCM Receivers," B.S.T.J., *53*, No. 9 (November 1974), pp. 1771–1793.
6. Y. Ueno, Y. Ohgushi, and A. Abe, "A 40 Mb/s and a 400 Mb/s Repeater for Fiber Optic Communication," Proceedings of the First European Conference on Optical Fiber Communication, 16–18 September 1975, IEEE Conference Publication, No. 132, pp. 147–149.
7. H. Melchior, A. R. Hartman, D. P. Schinke, and T. E. Seidel "Planar Epitaxial Silicon Avalanche Photodiode," B.S.T.J., this issue, pp. 1791–1807.
8. T. L. Maione and D. D. Sell, "Experimental Fiber-Optic Transmission System for Interoffice Trunks," IEEE Trans. Commun., *COM-25* (May 1977), pp. 517–522.
9. R. J. McIntyre, "Multiplication Noise in Uniform Avalanche Diodes," IEEE Trans. Electron Dev., *ED-13* (January 1966), pp. 164–168.
10. H. Melchior and A. R. Hartman, "Epitaxial Silicon n^+-p-π-p^+ Avalanche Photodiodes for Optical Fiber Communications at 800 to 900 Nanometers," Technical Digest IEDM Meeting, Washington, D.C., 1976, pp. 412–415.
11. R. J. McIntyre, "The Distribution of Gains in Uniformly Multiplying Avalanche Photodiodes: Theory," IEEE Trans. Electron Dev., *ED-19* (June 1972), pp. 703–713.
12. J. Conradi, "The Distribution of Gains in Uniformly Multiplying Avalanche Photodiodes: Experimental," IEEE Trans. Electron Dev., *ED-19* (June 1972), pp. 713–718.
13. S. D. Personick, P. Balaban, J. H. Bobsin, and P. Kumer, "A Detailed Comparison of Four Approaches to the Calculation of the Sensitivity of Optical Fiber System Receivers," IEEE Trans. Commun., *COM-25* (May 1977), pp. 541–548.
14. P. Balaban, "Statistical Evaluation of the Error Rate of the Fiberguide Repeater using Importance Sampling," B.S.T.J., *55*, No. 6 (July–August 1971), pp. 745–766.
15. P. W. Shumate, Jr., F. S. Chen, and P. W. Dorman, "GaAlAs Laser Transmitter for Lightwave Transmission Systems," B.S.T.J., this issue, pp. 1823–1836.